doi:10.1038/nature10188

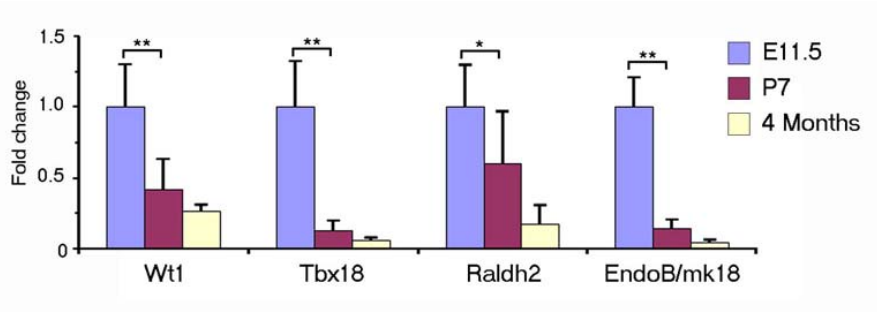

Supplementary Figure 1. Embryonic epicardial genes are down-regulated from mid-gestation stages and barely detectable post-natally.

Real time qRT-PCR revealed a significant down-regulation ($p^* \leq 0.05$; $p^{**} \leq 0.01$) of the epicardial genes *Wt1*, *Tbx18*, *Raldh2* and *EndoB* in intact hearts from embryonic E11.5 through to post-natal day 7 (P7) and 4 months of age. Wt1 is only expressed either transiently or at low levels in rare, isolated cells within the postnatal epicardium (data not shown). Bars represent mean $\pm$ s.e.m., N values are numbers of hearts analysed for each group: N=4 (E11.5 and P7), N=3 (4 months). All statistics Student's t-test.

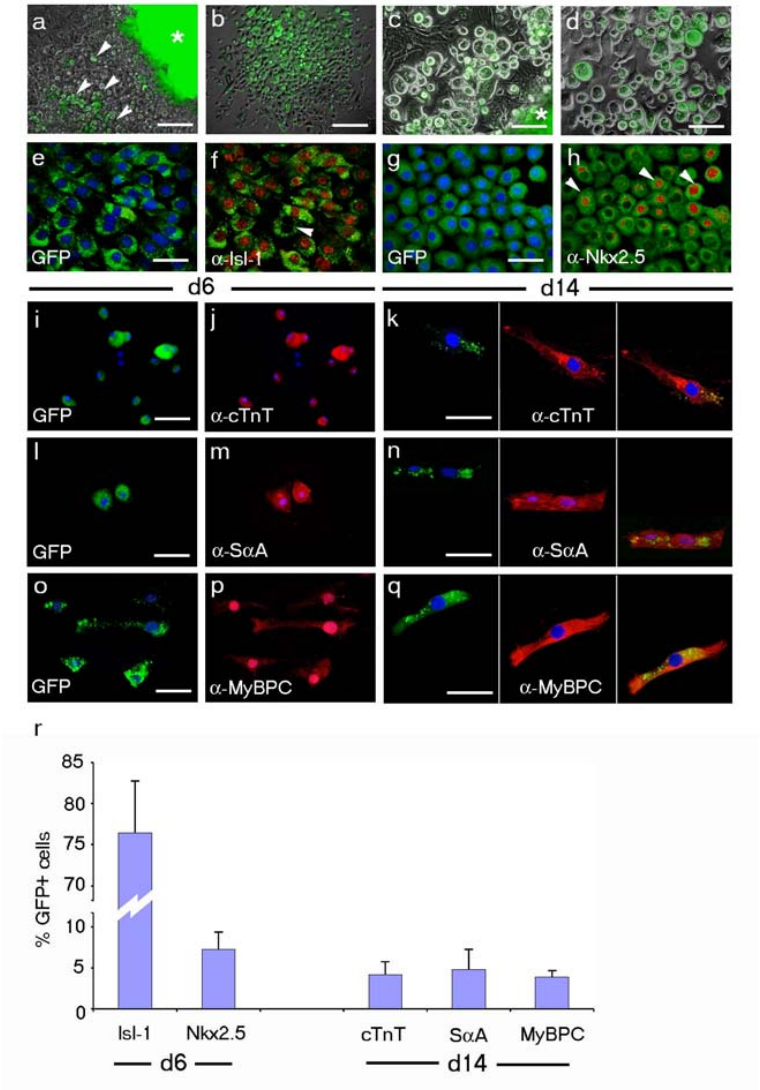

Supplementary Figure 2. Tβ4 primed Wt1+ cells give rise to cardiac progenitors ex vivo.

Primed GFP+ progenitors (white arrowheads) migrated from epicardial explants (explant highlighted by white asterisk; **a**). Clusters of migrating GFP+ cells (**b**) at higher magnification (white asterisk in **c**, **d**). GFP+ cells co-stained for Isl-1 (**e**, **f**; white arrowhead in **f** indicates an Isl-1 negative EPDC surrounded by an Isl-1+ cluster) and

Nkx2.5 (**g**, **h**; white arrowheads indicate Nkx2.5+ cells) provided evidence of cardiac progenitor formation. At day 6 of culture (d6) explant-derived GFP+ cells were observed which co-stained for cTnT (**i**, **j**), SαA (**l**, **m**) and MYBPC (**o**, **p**) as evidence of maturation of progenitors. Importantly, vehicle-treated cells failed to adopt a myocardial fate and only isolated fibroblast-derivatives were observed in control cultures (not shown). At day 14 (d14) derivatives were observed with more punctate GFP expression and evidence of cTnT+ (**k**), SαA+ (**n**) MYBPC+ (**q**) sarcomeric structure along with an elongated rod-shaped phenotype, indicative of mature cardiomyocytes. Cell quantification analysis revealed a significant % of GFP+ cells positive for Isl-1 with a relatively smaller % positive for Nkx2.5 at d6. At d14 a significant % of GFP+ cells also positive for the cardiomyocyte differentiation markers cTnT, SαA and MYBPC was detectable (**r**). Scale bars in **a**, **m**, **n**, **q** represent 100μm; in **c** represents 500μm and in **c**, **d**, **e**, **g**, **i**, **l** and **o** represent 50μm. Bars represent mean ± s.e.m., N values are numbers of cultures analysed for each group: N=4 (d6 and d14).

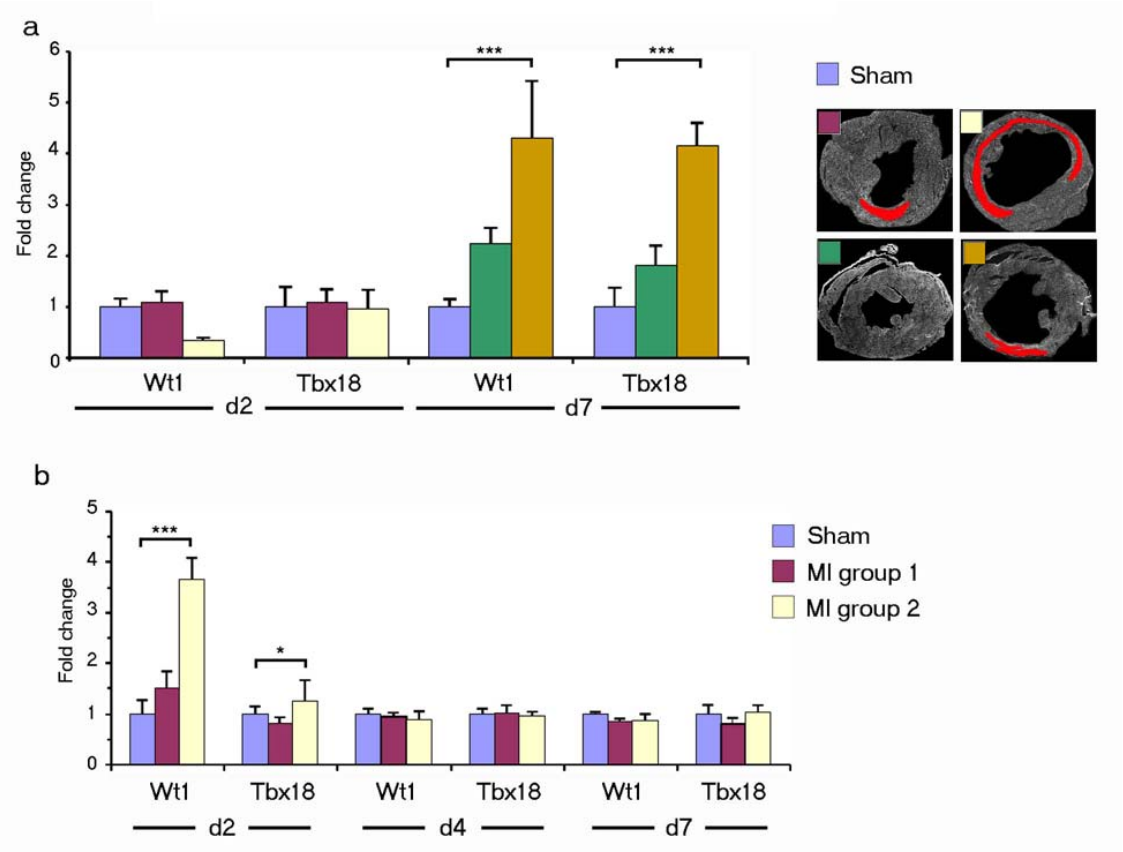

Supplementary Figure 3. Injury and Tβ4 priming reactivate embryonic epicardial gene expression in the adult heart.

After MI alone *Wt1* and *Tbx18* were significantly increased by day 7 post-injury relative to sham operated control hearts (p***≤0.001) with the up-regulation in expression dependent upon severity of injury: histogram key illustrates short axis sections through representative injured hearts/per injury group (d2: purple=mild injury; cream=severe injury; d7: green=mild injury; yellow=severe injury) with extent of injury highlighted in red (n=4 hearts per injury category per day post-MI) (**b**). Tβ4 priming resulted in a precocious (relative to injury alone) up-regulation in *Wt1* (p***≤0.001) and *Tbx18* (p*≤0.05) as early as day 2 post-MI, dependent upon severity of injury (categories: purple=mild injury; cream=severe injury; n=4 hearts per MI group. Representative sections shown in **b**), with levels of both genes returned to sham-operated control levels at day 4 through to day 7 post-MI (**c**). Bars represent mean ± s.e.m., N values are numbers of hearts analysed for each group: N=2 (**a**, **b**). All statistics Student's t-test.

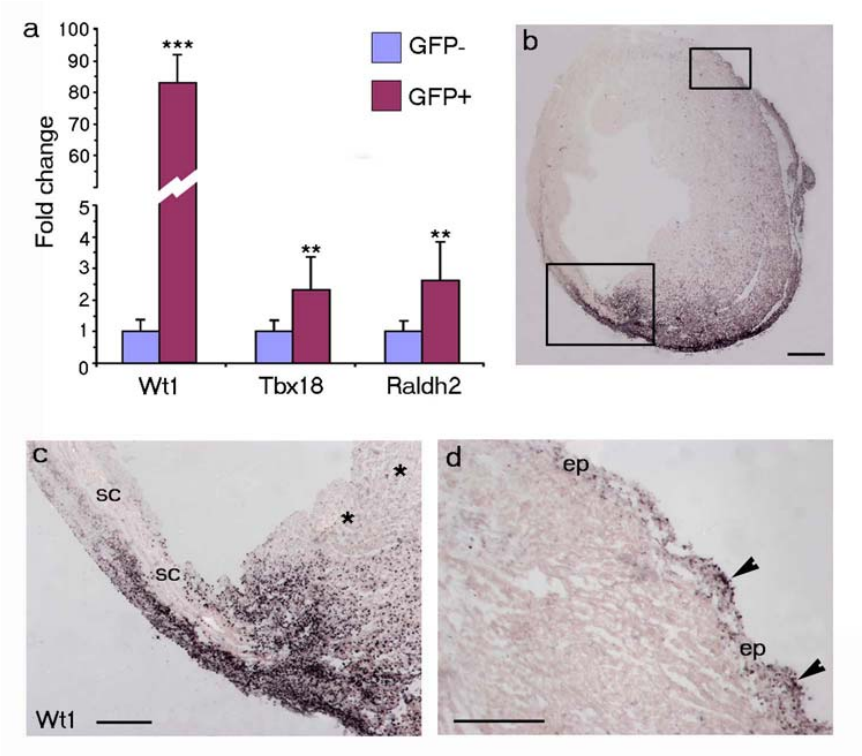

Supplementary Figure 4. Up-regulation of embryonic epicardial gene expression in Tβ4/injury primed FACS isolated GFP+ progenitors and activated *Wt1* in situ post-MI.

qPCR analyses on progenitors isolated by FACS from the hearts of Wt1-GFP animals at day 4 post-Tβ4 treatment and MI revealed significant up-regulation in *Wt1*, *Tbx18* and *Raldh2* relative to the GFP- fraction (**a**). In situ hybridisation for *Wt1* on sections through Tβ4-treated hearts at day 4 post MI (**b**), revealed a significant increase in *Wt1* expressing cells residing in the epicardium and sub epicardial region proximal to the scar whereas areas of non-*Wt1* expressing cells could be distinguished in the underlying myocardium (highlighted by black asterices; **c**). In remote myocardium, Wt1 expression was confined to the epicardium post-Tβ4/injury (highlighted by black arrowheads; **d**). Black boxes in **b**, are shown at high power in **c** and **d**. Scale bar in **b**, represents 1mm; **c** and **d** represents 500μm. ep, epicardium, sc, scar. Bars represent mean ± s.e.m., N values are numbers of hearts analysed for each group: N=6 (**a**); p**≤0.01, p***≤0.001; all statistics Student's t-test.

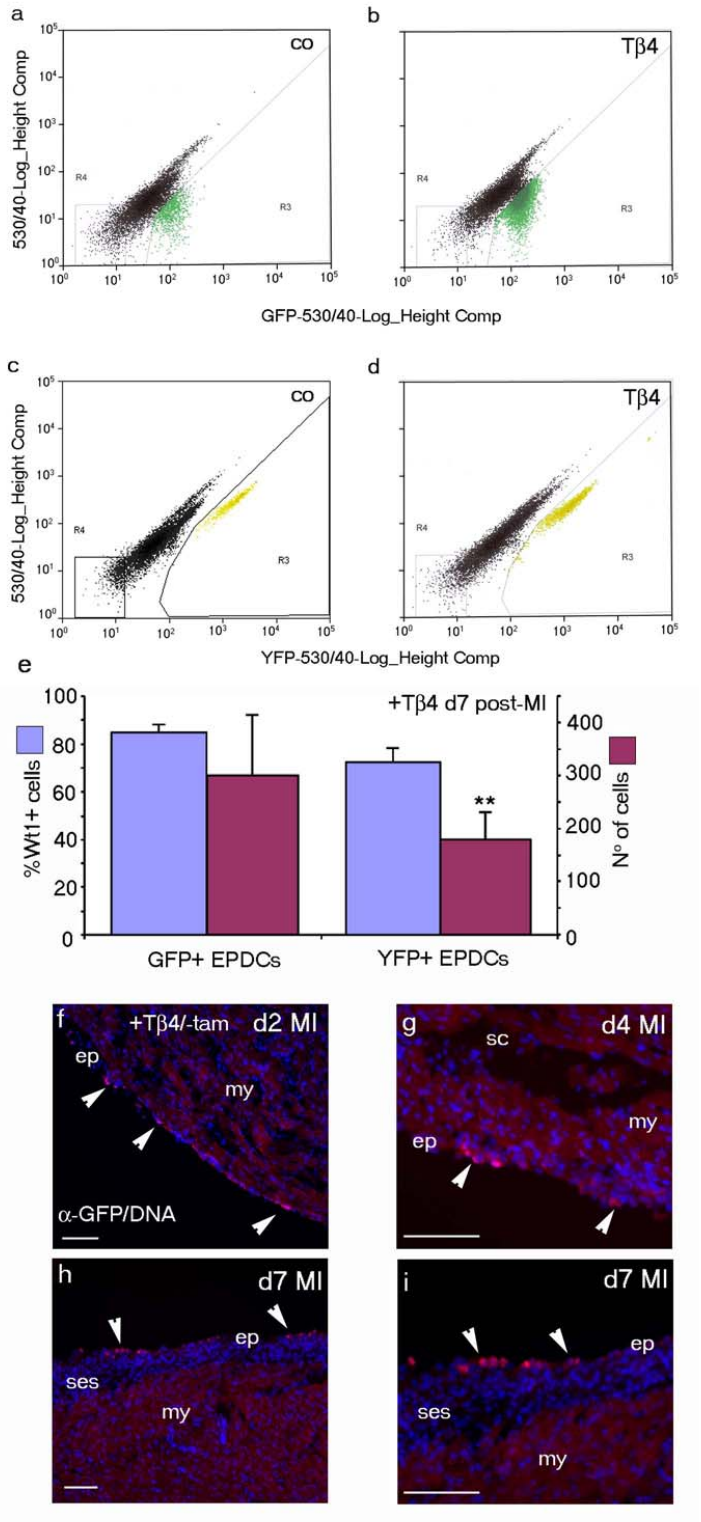

Supplementary Figure 5. Elevated numbers of GFP+ and YFP+ Progenitors in whole hearts following Tβ4 priming and injury relative to Tβ4-primed without tamoxifen controls.

FACS analyses scatter plots of GFP+ (**a, b**) and YFP+ (**c, d**) at day 7 post-MI following priming of Wt1-GFP and Wt1-ERT2YFP mice, respectively, with PBS vehicle (co; **a, c**) or Tβ4 (**b, d**). Note injury alone resulted in a modest detection of both GFP+ and YFP+ cells (**a, c**) and the numbers of both GFP+ and YFP+ cells were significantly augmented by Tβ4 priming (GFP+ and YFP+ $p \leq 0.001$; n=3 hearts per PBS versus Tβ4 treatment). P-values calculated by Student's t-test. Analyses of GFP+ and YFP+ cell counts, detected by α-GFP immunostaining at day 7, revealed a reduced number of YFP+ cells relative to GFP+ cells in situ (** $p \leq 0.01$), however, the % of Wt1+ cells within each labelled population was equivalent (**e**). A reduced frequency of pulse-labelled YFP+ cells, compared to constitutively labelled GFP+ cells, is consistent with that observed in the developing heart[4] and likely due to inefficient CreERT2 activation by tamoxifen when administered at non-toxic concentrations. An important further control with respect to the Wt1-ERT2YFP model was PBS-treatment or Tβ4-priming in the absence of tamoxifen. This resulted in an expected failure to flow sort YFP+ cells (data not shown) and confirmed Tβ4 priming did not result in a non-specific cellular recombination. In Wt1-ERT2YFP hearts primed with Tβ4, but without tamoxifen treatment, we were unable to flow sort YFP+ cells but observed rare, isolated YFP+ cells in the epicardium in response to injury, at day 2 post-MI as detected by α-GFP immunostaining (**f;** YFP+ cells highlighted throughout by white arrowheads). The YFP+ cells remained in the epicardium through to days 4 (**g**) and 7 post-MI (**h**, **i**); without migrating into the underlying subepicardial space or myocardium and failed to differentiate into cardiovascular derivatives (**i**). ep, epicardium; my, myocardium; ses, subepicardial space. Scale bars **f-i** represent 100 μm. Bars represent mean ± s.e.m., N values are numbers of hearts analysed for each group: N=9 (GFP+) and N=6 (YFP+) (**e**). All statistics Student's t-test.

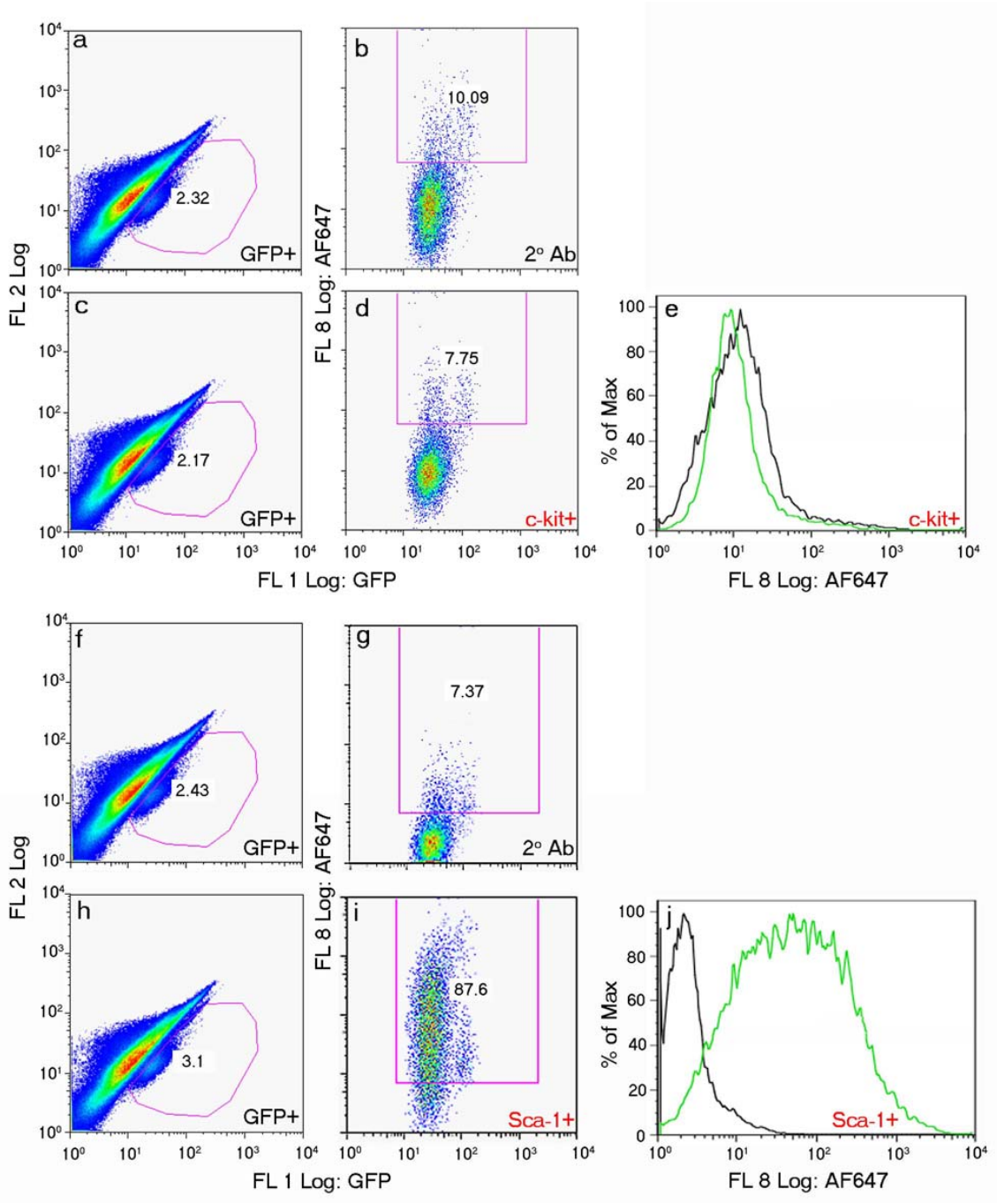

Supplementary Figure 6. Tβ4/injury responsive progenitors are c-kit negative but contain a significant Sca-1 positive sub-fraction.

Single cell suspensions from hearts of $Wt1^{GFPCre/+}$ mice treated with Tβ4 were prepared

by enzymatic digestion 4 days post-MI and incubated with antibodies against the stem cell markers, c-kit (**a-e**) or Sca-1 (**f-j**) and analyzed by flow cytometry. Scatter plots revealed GFP+ cells (**a**, **c, f, h**) which were negative for c-kit relative to secondary antibody alone (**b**, **d**) but revealed a significant sub-fraction (~80%) which were positive for Sca-1 relative to background (**g, i**). The c-kit negative and Sca-1 positive GFP+ populations were also plotted in the representative histograms showing relative number of cells (% Max) expressing the relevant level of signal. Cells incubated with secondary antibody alone, as a negative control, are shown in black and cells incubated with antibodies against c-kit and Sca-1 are shown in green (**e**, **j**).

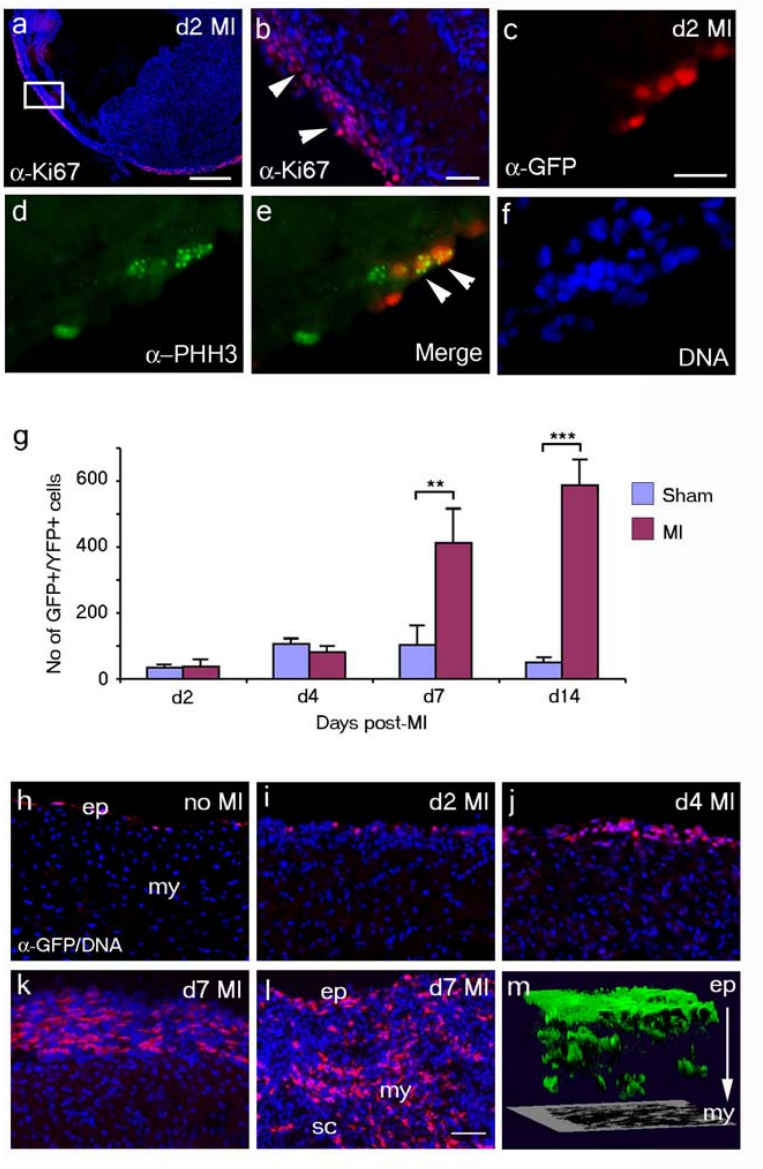

Supplementary Figure 7. Proliferation and expansion of GFP+ and YFP+ cells within the epicardium and sub-epicardial regions following Tβ4 priming/injury.

Ki67+ cells, at low magnification (**a**) and higher magnification of white box inset (**b**), proliferated within the epicardium and subepicardial regions (highlighted by white arrowheads in **b**) after 2 days post-MI when primed by Tβ4. YFP+ cells (**c**) co-stained for

PHH3 (**d**, **e**) proliferated within the epicardium (white arrowheads in **e**) after Tβ4/injury priming (**c-f**). Cell quantification reveled an increase in total numbers of GFP+ and YFP+ cells with injury compared to sham operated control hearts from days 2, 4, 7 ($p^{**} \leq 0.01$) to day 14 ($p^{***} \leq 0.001$ post-MI; n=4 hearts per sham and MI group; **g**). Total cell number increased over time as verified by spatiotemporal immunostaining with α-GFP. Rarely were YFP+ cells detectable in the absence of injury and were spatially restricted to the epicardium (**h**). Progressive increases in YFP+ cells were observed across days 2, 4 and 7, with evidence of migration into the underlying myocardium (**i-k**). YFP+ cells were detected throughout the myocardium in regions proximal to the site of injury and scar (**l**). Multi-photon-derived 3D reconstructions revealed the extent of migration of YFP+ progenitors from the epicardial surface to underlying myocardium in response to injury and Tβ4 (**m**). Scale bar in **a** represents 1mm; **b** represents 50μm **c**, represents 50μm applies to **c-f**; **l** represents 50 μm applies to **h-l**. ep, epicardium, my, myocardium; sc, scar region. Bars represent mean ± s.e.m., N values are numbers of hearts analysed for each group: N=4 (d2 and d4) and N=7 (d7 and d14) (**g**). All statistics Student's t-test.

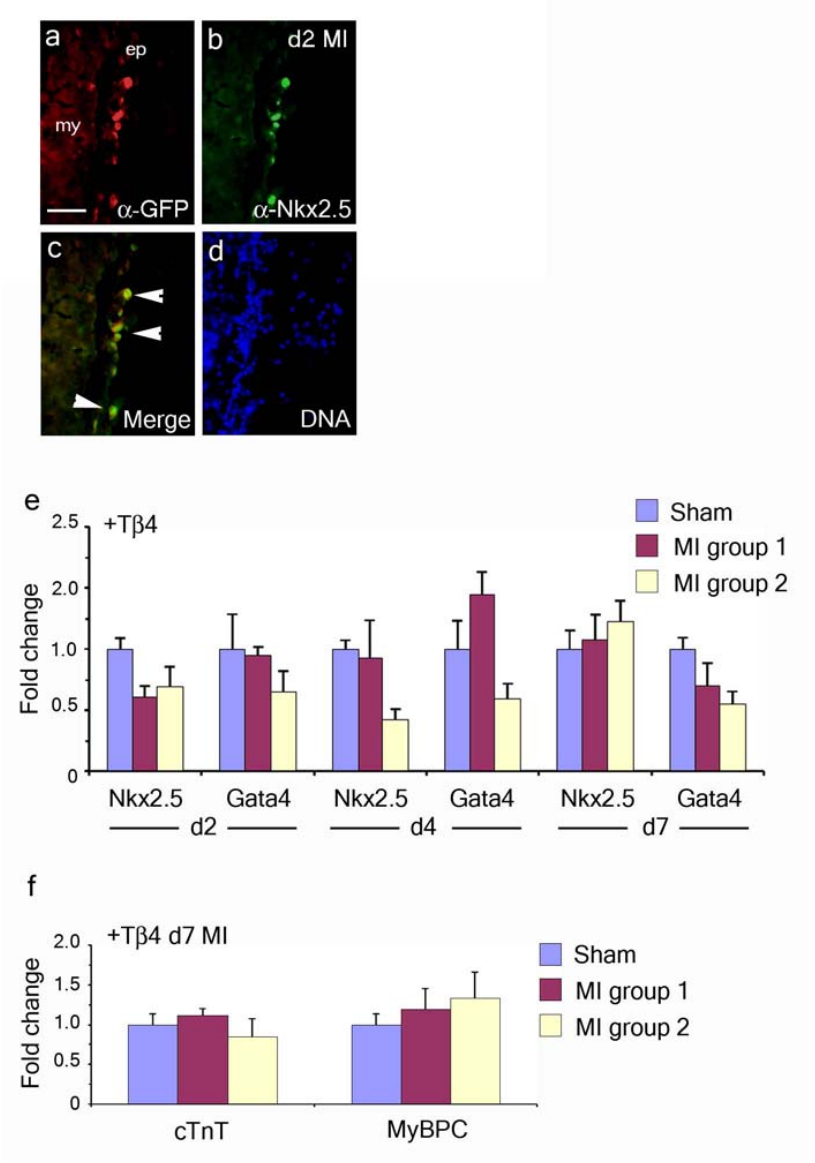

Supplementary Figure 8. Evidence of Nkx2.5+/YFP+ cardiac progenitors.

Immunostaining with α-GFP (**a**) and α-Nkx2.5 (**b**) revealed double positive cells (**c;** highlighted by white arrowheads) residing in the epicardium 2 days post-MI, indicative of Wt1+-derived cardiac progenitors in response to Tβ4/injury priming. Note the cells

residing in the epicardium have large nuclei relative to their cytoplasm as is common to progenitor populations (see merge in **c** highlighting GFP+ cytoplasm against GFP+/Nkx2.5+ nuclei). Real time qRT-PCR analyses failed to reveal increases in *Nkx2.5* or the additional early cardiac progenitor marker *Gata4* across days 2, 4 and 7 post-MI (categories: blue=sham operated controls; purple=mild injury; cream=severe injury; n=4 hearts per group, representative sections as for Supplementary Fig. 1b) despite the evident increase in progenitor cell numbers (see Fig. 2**m**) (**e**). Similarly qRT-PCR did not reveal any change in markers of mature cardiomyocytes, cTnT or MyBPC at day 7 post-MI despite evidence of the addition of de novo YFP+ cells staining positive for cTnT (Fig. 3**f**, **g**) (**f**). The lack of increase in expression of early and late cardiac markers when measured across the entire heart reflects the pre-existing high levels of these genes in resident myocardium, masking the effect of a contribution via de novo progenitor/myocytes. Scale bar in **a** represents 50μm and applies to **a**-**d**. ep, epicardium; my, myocardium. Bars represent mean ± s.e.m., N values are numbers of hearts analysed for each group: N=2 (**g, f**).

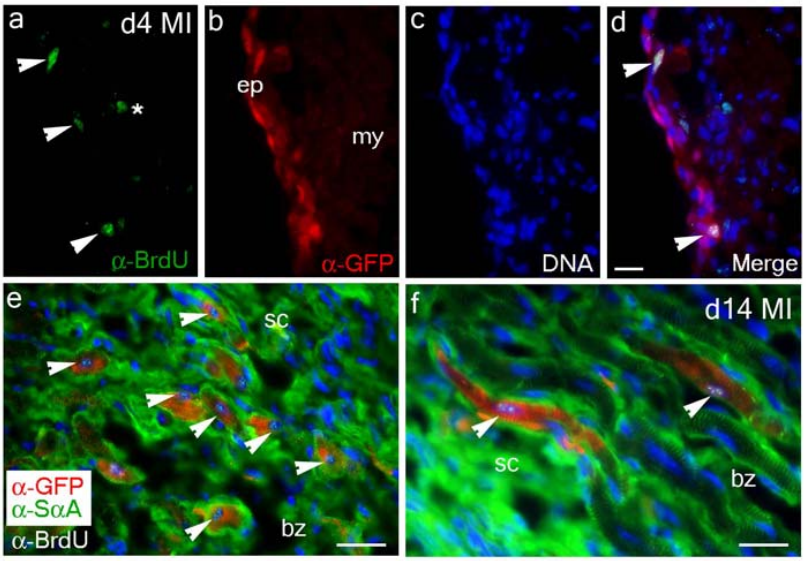

Supplementary Figure 9. BrdU pulse chase identifies mitotically active GFP+ progenitors at day 4 traced to BrdU+/GFP+ cardiomyocytes at day 14 post-MI.

Sections through hearts of $Wt1^{GFPCre/+}$ animals injected with BrdU on days 0, 2 and 4 post-MI revealed BrdU+ progenitor-like cells residing in the epicardium at day 4 as determined by α-BrdU immunostaining (**a**) which were also GFP+ as determined by α-GFP immunostaining (**b**). White arrowheads in (**a**) highlight BrdU+ cells located in the epicardium, which were positive for GFP as indicated in (**d**); white asterisk in (**a**) indicates a cell positive for BrdU located in underlying myocardium which was GFP-. At day 14 post-MI BrdU+ cardiomyocytes, by virtue of staining for SαA, were detected within the myocardium, residing in the border zone and scar region, which were also GFP+ (**e**; as highlighted by white arrowheads). Higher magnification view of two BrdU+/GFP+ cells in the scar region with evident sarcomeric banding as an indicator of a mature cardiomyocyte phenotype (**f;** as highlighted by white arrowheads). bz, border zone; ep, epicardium; my, myocardium; sc, scar. Scale bars in **d** represents 20μm, in **e** represents 50 μm and in **f** represents 20μm..

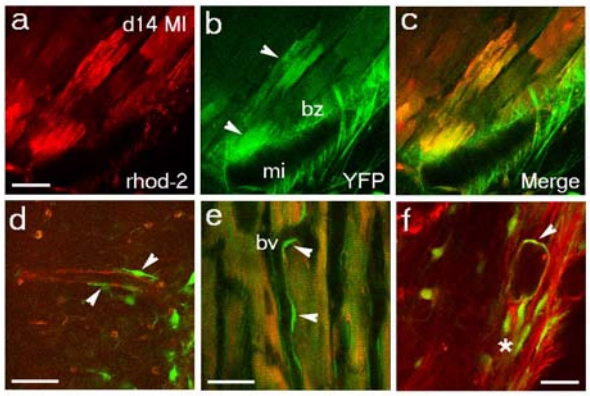

Supplementary Figure 10. YFP+ EPDC-derivatives residing in the border zone of injury and associated with coronary vessels.

Multi-photon imaging and rhod-2 loading at day 14 post-MI (**a**) revealed Tβ4-primed "maturing" YFP+ rod-shaped cells, which did not support calcium transients, residing in the border zone of injury (white arrowheads highlight YFP+ cells; **b**). Merge of YFP+/rhod-2 illustrates disrupted fibres (green) at site of injury (**c**). YFP+ cells were observed in close proximity to and/or contributing to coronary vessels (**d-e**) with putative pericyte-like (**d**, **e**; highlighted by white arrowheads), endothelial-like (white arrowhead; **f**) or fibroblast-like appearances (based on cell morphology and localization; white asterisk highlights cell cluster; **f**). Scale bars in **a** and **f** represent 20 μm; scale bars in **d** and **e** represent 10 μm. bv, blood vessel; bz, border zone; mi, myocardial infarction.

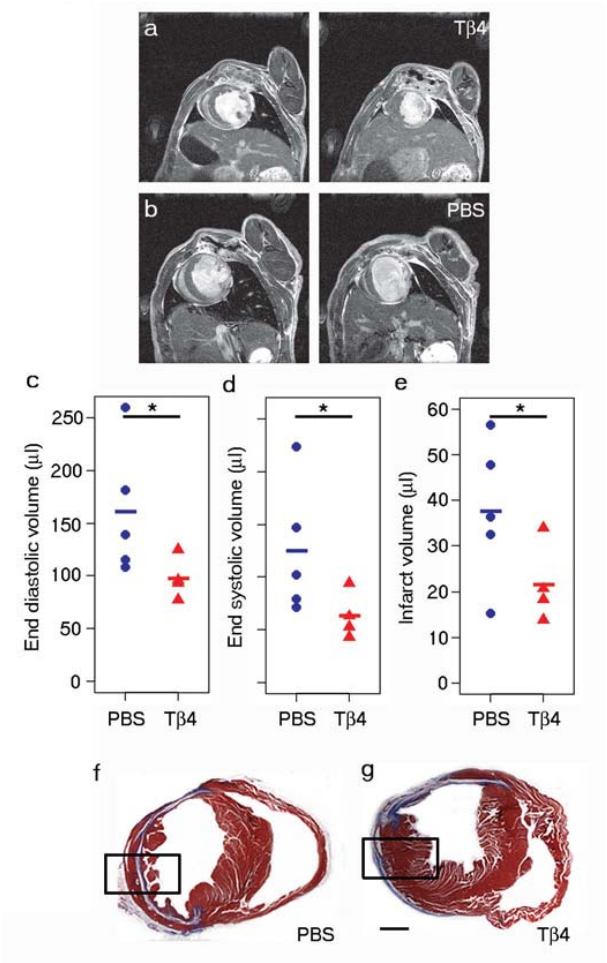

Supplementary Figure 11. Wt1+ progenitor-derived cardiomyocytes contribute to improved cardiac output and myocardial regeneration.

MRI analyses with representative short axis images (mid ventricular slice and one slice 1.5 mm offset towards the apex) of infarcted hearts 28 days after surgery with late gadolinium enhancement following treatment with either Tβ4 (**a**) or PBS (**b**). Infarcted myocardium (scar tissue) appears bright on late gadolinium enhancement images due to gadolinium accumulation. Scatter plots for end diastolic volume (EDV; **c**), end systolic volume (ESV; **d**) and infarct volume (**e**) for PBS (blue, n=5) and TB4 (red, n=4) treated animals 28 days after surgery. The horizontal bars indicate the means for each group. All three parameters were significantly lower in TB4-treated versus PBS-treated groups indicative of reduced scarring, remodeling and increased cardiac function. At the early time point, 7 days post-MI, we observed an increase in ejection fraction (EF) in Tβ4 treated animals (36 $\pm$ 4%) compared to the control PBS treated group (27 $\pm$ 6%). This was consistent with an early role for Tβ4 in maintaining cardiomyocyte survival as

previously reported (Supplementary Table 1). Measurements at 28 days post-MI revealed end diastolic volumes (EDV) and end systolic volumes (ESV) for PBS treated animals (EDV, 173.9 ± 28.4µl and ESV, 138.1 ± 28.6 µl; n=5) which were significantly higher compared to Tβ4 treated animals (EDV, 89.8 ± 5.1µl; n=4, $p \leq 0.05$ and ESV ,52.8 ± 5.0µl; n=4, $p \leq 0.05$; **c, d**)). These data revealed significantly reduced pre- and after-loading, respectively, on the injured heart with Tβ4 treatment, which was progressively lowered over time (Supplementary Table 1). Reduction in loading represented a prelude to decreased ventricular distension and remodelling (**a, b**) and a significant improvement in ejection fraction (EF) in the TB4 treated animals (41 ± 3%; n=4) compared to the PBS treated controls (23 ± 3%; n=5; $p \leq 0.01$; repeated measures one way ANOVA; Supplementary Table 1). Scar volume, as assessed via late gadolinium enhancement, was significantly higher in PBS treated mice (43.3 ± 4.9µl; n=5) compared to those that received TB4 (22.0 ± 5.3µl; n=4; $p \leq 0.05$), suggesting that the Tβ4 priming reduced infarct volume (**e**). In addition, % infarct relative to LVM was significantly reduced in Tβ4 treated (18 $\pm$ 4%; n=4) as compared to PBS treated (27 $\pm$ 2; n=5; $p \leq 0.05$) animals (Supplementary Table 1) indicating that Tβ4-priming not only reduced scarring but also increased ventricular myocardial mass. LVM can be interpreted as an index of hypertrophy, with respect to normal pathology post-MI, but when viewed in the context of reduced infarct volume and % scarring may indicate increased myocardial cell number. Trichrome stained transverse sections (cut at the level of the ventricular papillary muscles) from PBS- (**f**) and Tβ4- (**g**) treated hearts, 28 days post MI; red represents viable myocardium and blue represents collagen deposition indicative of scarring and fibrosis. Note the increased proportion of healthy myocardium highlighted by the black box in (**g**) relative to the comparative region in (**f**). * $p \leq 0.05$; all statistics by repeat measures one way ANOVA. Scale bar in **g** represents 1mm applies to **f**, **g**.

Supplementary Table 1. Functional cardiac parameters from MRI analyses of TB4 and PBS primed animals following MI

	7 days post surgery		14 days post surgery		28 days post surgery	
	TB4 (n=4)	**PBS** (n=5)	**TB4** (n=4)	**PBS** (n=5)	**TB4** (n=4)	**PBS** (n=5)
body weight [g]	27.0 ± 3.3	26.3 ± 0.9	28.1 ± 3.7	27.3 ± 0.8	27.4 ± 2.7	27.5 ± 0.9
heart rate [bmp]	552 ± 29	561 ± 11	558 ± 19	570 ± 27	547 ± 24	559 ± 13
left ventricle						
EDV [µl]	93.4 ± 11.6	135.2 ± 18.2	101.1 ± 15.0	153.3 ± 23.3	89.0 ± 5.1*	173.9 ± 28.4
ESV [µl]	61.2 ± 11.9	102.2 ± 21.5	67.9 ± 13.1	114.7 ± 25.6	52.8 ± 5.0*	138.1 ± 28.6
SV [µl]	32.2 ± 1.2	33.0 ± 3.7	33.2 ± 2.0	38.6 ± 2.7	36.2 ± 2.1	35.8 ± 0.4
EF [%]	36 ± 4	27 ± 6	34 ± 3	28 ± 5	41 ± 3**	23 ± 3
CO [ml/min]	17.8 ± 1.3	18.7 ± 2.4	18.5 ± 0.9	22.0 ± 2.0	19.9 ± 1.7	20.0 ± 0.5
LVM [mg]	129 ± 7	171 ± 10	132 ± 9	152 ± 10	128 ± 6	166 ± 7
infarct Vol. [µl]	29.2 ± 5.8	53.2 ± 10.0	28.1 ± 3.7	42.6 ± 7.2	22.0 ± 5.3*	43.3 ± 4.9
infarct [% LVM]	24 ± 5	32 ± 5	23 ± 4	29 ± 4	18 ± 4*	27 ± 2

#data presented as mean ± standard error of mean.

Asterices indicate significant differences between TB4 and PBS treated:* p≤0.05; **p≤0.01; repeated measures one way ANOVA.